

Determination of Activation Energy of Amorphous to Crystalline Transformation for Bi_2S_3 chalcogenide Glasses by Using Isoconversional Methods

¹Abdullah Omar Ali, ²Tawfik Mahmood Mohammed Ali, ^{3*}Mehdi Ahmed Dabban

^{1,3}Physics Department, Faculty of Science, University of Aden, Yemen

²Physics Department, Faculty of Education, University of Aden, Yemen

*Corresponding Author's E-mail: dabbanm@yahoo.com

Abstract - In this work, the structure and kinetics of the crystallization reaction of amorphous Bi_2S_3 chalcogenide glasses were investigated using powder X-ray diffraction, scanning electron microscopy (SEM), and differential scanning calorimetry (DSC) techniques under non-isothermal conditions with different heating rates (10-30 K/min). The DSC crystallization data is analyzed using the isoconversional models. The results revealed that the activation energy strongly depends on the rate of heating by applying the equivalent transformation method proposed by Kissinger-Akahira-Sunose (KAS), Flynn-Wall-Ozawa (FWO), Tang, Starink, and Vyazovkin. These modifications suggest that transforming from the amorphous to the crystalline phase in Bi_2S_3 chalcogenide glasses was a complicated process involving a variety of nucleation and growth mechanisms.

Keywords: Crystallization kinetics; Differential scanning calorimetry (DSC); Activation energy; Isoconversional methods.

1. Introduction

Bismuth sulfide (mineral *bismuthinite*) is a non-toxic semiconductor which possesses a lamellar structure joined together by weak Bi-S bonds. It is a crystalline n-type V-VI semiconductor material that belongs to the main group metal chalcogenides of the type $\text{A}_2\text{B}^{\text{VI}}$ (A = Sb, Bi, As; B = S, Se, Te) [i-ii]. It is one of such important materials whose band gap energy, 1.7 eV, lies in visible solar energy spectrum [iii-iv]. Semiconducting bismuth sulphide films have received considerable attention in recent years because of their range of applications: photoelectrochemical cells [v], thermoelectric cooling [vi] and metal sulphide thin film photography [vii].

Determination of kinetic parameters of chalcogenide glass crystallization kinetics using differential scanning calorimetry (DSC) technique is a very common method. One of the most important kinetic parameters that can be determined by DSC measurements is the activation energy E of crystallinity in the kinetics of the amorphous to crystalline transition. As stated by Vyazovkin [viii], it can provide useful information about the different mechanisms involved in the transformation process.

The crystallization kinetics of amorphous Bi_2S_3 alloy isn't sufficiently studied [ix]. To achieve this goal, the differential scanning calorimeter (DSC) method is used to study the kinetics of crystallization of amorphous Bi_2S_3 alloys at different constant heating rates. Analysis of the DSC data is carried out using the isoconversional methods in order to investigate the growth processes involved in the transformation. An analysis of the dependence of the activation energy of crystallization (E) on the heating rate is presented.

2. Theoretical aspects of thermal analysis

Model-free isoconversion methods are the most reliable methods for the calculation of the activation energy of thermally activated reactions [x-xiii]. A large number of isoconversion methods have been conducted for polymer materials, but only a few for studies on chalcogenide glasses. The solid-state rate of conversion $d\alpha/dt$, described by the rate constant $k(T)$ and reaction model $f(\alpha)$ which is dependent on the solid-state reaction model (Table 1), is given by:

$$\frac{d\alpha}{dt} = k(T)f(\alpha), \quad (1)$$

Where $k(T)$ is the reaction rate constant, which depends on temperature (T), and $f(\alpha)$ is the reaction model, which depends on conversion (α). The value of $f(\alpha)$ indicates the volume of the crystalline fraction.

Table 1: Algebraic expressions of $f(\alpha)$ for the kinetic models considered in this work in the solid state reactions [xiv]

Reaction Model	Symbol	$f(\alpha)$
Zero-order (Polanyi-Winger equation)	R1	1
Phase-boundary controlled reaction (contracting area, i.e., bidimensional shape)	R2	$2(1-\alpha)^{1/2}$
Phase-boundary controlled reaction (contracting volume, i.e., tridimensional shape)	R3	$3(1-\alpha)^{2/3}$
First-order (Mampel)	F1	$(1-\alpha)$
Johnson-Mehl-Avrami	JMA(n)	$n(1-\alpha)[- \ln(1-\alpha)]^{1-\frac{1}{n}}$
Sestak-Berggren	SB(M,N)	$\alpha^M (1-\alpha)^N$
Reaction Order	RO(N)	$(1-\alpha)^N$
One-dimensional diffusion	D1	$1/2\alpha$
Two-dimensional diffusion (bidimensional particle shape) Valensi equation	D2	$-[1/\ln(1-\alpha)]$
Three-dimensional diffusion (tridimensional particle shape) Jander equation	D3	$(1.5)(1-\alpha)^{1/3} / [(1-\alpha)^{-1/3} - 1]$
Three-dimensional diffusion (tridimensional particle shape) Ginstling-Brounshtein	D4	$(1.5)[(1-\alpha)^{-1/3} - 1]$

The first part of equation (1) usually exhibits an Arrhenian temperature dependence, as shown in equation (2):

$$k = A e^{(-E/RT)}, \tag{2}$$

Where A (s^{-1}), E ($kJ\ mol^{-1}$) and R ($8.314\ J/mole\ K$) are the pre-exponential (frequency) factor, the activation energy, and the universal gas constant, respectively. Therefore, Eq. (2) can be written as:

$$\frac{d\alpha}{dt} = A e^{(-E/RT)} f(\alpha) \tag{3}$$

There is a wide range of theoretical models and mathematical treatments to estimate the activation energy of a reaction. These models can be categorized into the two most popular (linear) and (non-linear) methods, as described below.

2.1 Isoconversion methods

Under non-isothermal conditions with a constant heating rate of $\beta = dT / dt = const.$, Eq. (3) may be rewritten as:

$$\frac{d\alpha}{dT} = \frac{A}{\beta} e^{\left(\frac{-E}{RT}\right)} f(\alpha) \tag{4}$$

Separating variables can be used to integrate Eq. (4) [xv];

$$\int_0^\alpha \frac{d\alpha}{f(\alpha)} = \frac{A}{\beta} \int_{T_0}^T e^{\left(\frac{-E}{RT}\right)} dT \approx \frac{AE}{\beta R} \int_{y_f}^\infty \frac{e^{(-y)}}{y^2} dy \tag{5}$$

Where T_0 is the initial temperature, $y = E/RT$ and T is the temperature at an equivalent (fixed) state of transformation. The integral on the right hand side is usually called the temperature integral, $P(y)$ and does not have analytical solution.

$$p(y) = \int_{y_f}^{\infty} \frac{e^{(-y)}}{y^2} dy \quad (6)$$

To solve the temperature integral Eq. (6), several approximations were introduced. In general, all of these approximations lead to a direct isoconversion (linear) method in the form of:

$$\ln\left(\frac{\beta_i}{T_{ai}^k}\right) = C - \frac{E_\alpha}{RT_{ai}} \quad (7)$$

The subscript i denotes different heating rates. For each degree of the conversion fraction, α , a corresponding T_{ai} and heating rate β are used to plot $\ln(\beta_i/T_{ai}^k)$ against $1/T_{ai}$. The plot should be a straight line whose slope can be used to calculate the activation energy E_α . However, the most popular models used for calculation of activation energy are:

- 1) The Kissinger-Akahira-Sunose (KAS) method [xvi-xvii], which takes the form:

$$\ln\left(\frac{\beta_i}{T_{ai}^2}\right) = C_K(\alpha) - \frac{E_\alpha}{RT_{ai}} \quad (8)$$

- 2) The Flynn-Wall-Ozawa (FWO) method, suggested independently by Flynn and Wall [xviii] and Ozawa [xix]. This method is given by:

$$\ln(\beta_i) = C_W(\alpha) - 1.0518 \frac{E_\alpha}{RT_{ai}} \quad (9)$$

- 3) The Tang method. A more precise formula for the temperature integral has been suggested by Tang *et al* [xx], which can be put in the form:

$$\ln\left(\frac{\beta_i}{T_{ai}^{1.894661}}\right) = C_T(\alpha) - 1.00145033 \frac{E_\alpha}{RT_{ai}} \quad (10)$$

- 4) The Starink method [16, 33], another new method, which is given by:

$$\ln\left(\frac{\beta_i}{T_{ai}^{1.92}}\right) = C_S(\alpha) - 1.0008 \frac{E_\alpha}{RT_{ai}} \quad (11)$$

2.2 The Vyazovkin method

A second way of extracting the same information is by using the advanced isoconversional method (non-linear) developed by Vyazovkin [xxi]. This method is a non-isothermal method that presents an accurate approximation of temperature integral, $P(y)$, which leads to:

$$\Omega = \sum_{i=1}^n \sum_{j \neq i}^n \frac{I(E_\alpha, T_{ai})\beta_j}{I(E_\alpha, T_{aj})\beta_i} \quad (12)$$

Where n is the number of experiments carried out at different heating rates. The activation energy can be determined at any particular value α by finding the value of E_a which minimizes the objective function Ω . The temperature integral (I) can be evaluated using an approximation suggested by Gorbachev [29]:

$$I = \int_0^T e^{-\frac{E}{RT}} dT = \frac{RT^2}{E + 2RT} e^{-\frac{E}{RT}} \quad (13)$$

3. Experimental

Bulk material was prepared by the well-established melt-quench technique. The high purity (99.999%) Bi, and S in desired stoichiometric ratios were sealed in a quartz glass ampoule under a vacuum of 10^{-5} Torr. The sealed ampoule was heated in controlled Furnace at 1200 K for 24 h. Through the heating process, the ampoules were frequently shaken to assure the homogeneity of molten materials. After achieving the desired time, the ampoules containing the molten materials were rapidly quenched in a mixture of ice and water. The ingots of the glassy samples were taken out by breaking the ampoules and then grinded to obtain them in powder to be used in the measurements.

The non-crystalline state of the investigated glasses was examined using X-ray diffractometer (Philips type 1710 with Cu as a target and Ni as a filter, $\lambda = 1.5418 \text{ \AA}$). The chemical composition of the films was studied using the standard energy dispersive analysis of X-ray (EDX) technique. An EDX unit attached to the scanning electron microscope (SEM), Jeol (JSM)-T200 type, was used for these measurements.

The differential scanning calorimetry, DSC was carried out on ~ 5 mg of powder samples to investigate the crystallization kinetics of Bi_2S_3 glass. The samples were sealed in standard pan and scanned over a temperature range from 360 to about 650 K at constant heating rates (10, 15, 20, 25, and 30 K/min) using a Shimadzu DSC-60 with a sensitivity of $\pm 10 \mu\text{W}$. The accuracy of the heat flow is $\pm 0.01 \text{ mW}$ and the temperature precision is determined by the microprocessor of the thermal analyzer is $\pm 0.1 \text{ K}$. The equipment was calibrated for temperature and enthalpy with Indium at the heating rate 10 K/min ($T_m = 156.6 \text{ C}$, $\Delta H_m = 28.55 \text{ J/g}$). The DSC experiments were conducted under a dry N_2 flow rate of 30 ml/min. The sample was pre-annealed at a temperature below the glass transition temperature. The condition of site saturation could be fulfilled to get information about the growth mechanism separately from the nucleation process. The glass transition, onset of crystallization and crystallization peak temperature were determined with accuracy $\pm 1 \text{ K}$ by using the microprocessor of the thermal analyzer. In order to ensure the reproducibility, most of the experiments repeated more than one time, and all used apparatuses were well calibrated using standard references before the measurements.

4. Results and Discussion

4.1 Structural studies

Fig. 1(a) depicts an EDX examination of the powder sample, which produced an average atomic percentage of Bi:S of 38.53:61.33, which is quite close to our target. Additionally, there was carbon present, which was utilized to seal the samples. The XRD pattern of Bi_2S_3 glass is shown in **Fig. 1(b)**. As shown, the pattern has no sharp lines, indicating that the as-prepared samples are amorphous. In **Fig. 1(c)**, conchoidal profiles with parallel ribs emphasize the glassy nature of the sample.

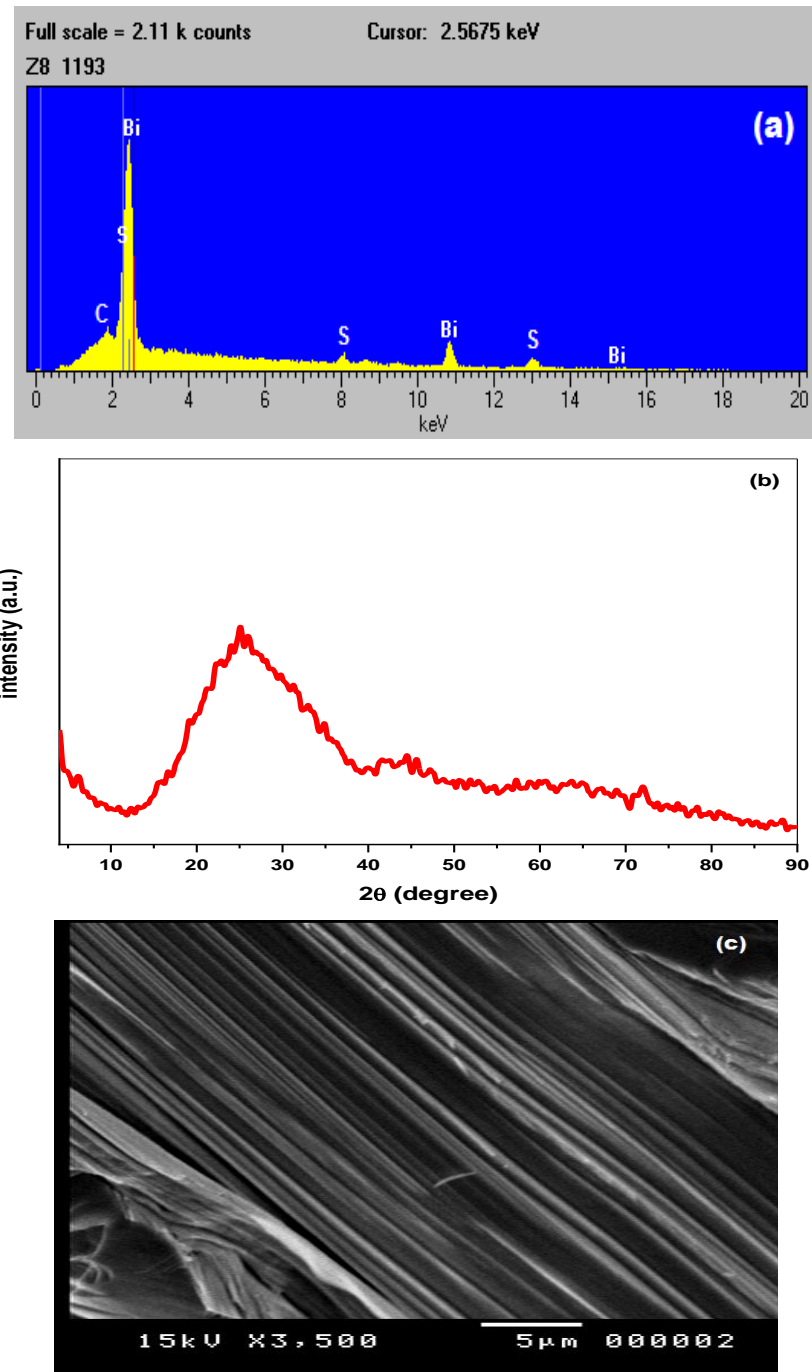


Fig. 1: (a) (EDX) spectrum (b) XRD pattern, and (c) SEM image of the Bi_2S_3 bulk glass

In order to infer the thermal properties of the bulk material under study, we have to measure the heat flow as a function of absolute temperature in the range of 350 to 750 K. Such thermal measurements in the aforementioned thermal range are sufficient to provide clear information on vitrification (glass transition) and crystallization regions, as well as regions where bulk material begins to melt. Thermal measurements were performed on the examined large sample at four heating rates ranging from 10 to 30 K/min (see Fig. 2 a,b). This figure reflects heat flow with respect to temperature, and the figure represents endothermic heat flow and exothermic heat flow, respectively. Within this thermal range, we distinguish four temperatures: the glass transition temperature T_g , the crystallization onset temperature T_c , the maximum crystallization temperature T_p , and the melting temperature T_m . It is clear from Table 1 that all of these temperatures increase with increasing heating rates. The higher the thermal heating rate, the more clearly observable the thermal activity of the material, which makes it suitable for use in many different applications. Our focus will be on the regions of glass transition and crystallization shown in Fig. 2b.

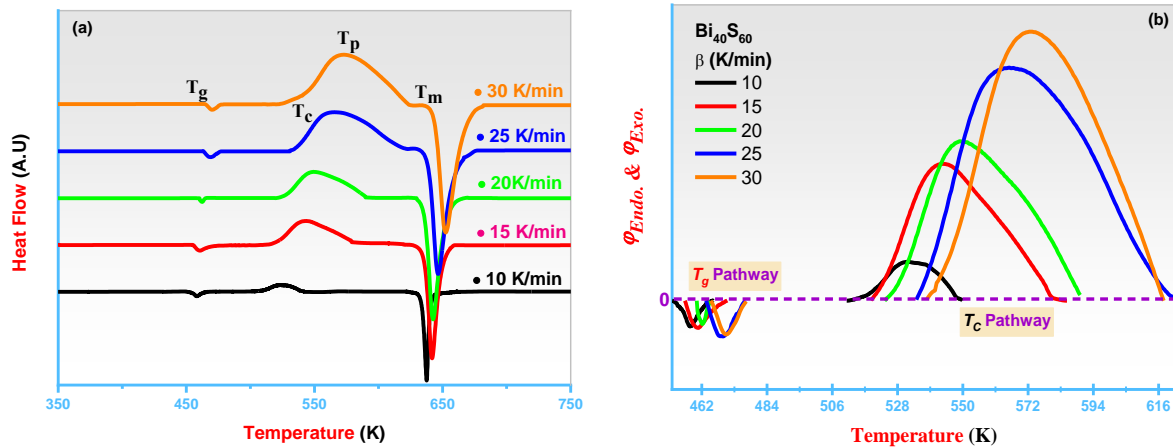


Fig. 2: (a) Full heat flow versus temperature and (b) (exothermic/ endothermic heat flow) versus temperature for the Bi_2S_3 bulk sample

Table 2: Thermal characteristic temperatures according to the heat flow-temperature trajectories of the Bi_2S_3 bulk alloy at different heating rates

β (Heating Rate)	T_g (K)	T_c (K)	T_p (K)	T_m (K)	ΔT (K)	H	H_r	S	K	T_g/T_m
10	451.00	508.00	523.46	637.59	57.00	0.126	0.499	1.95	0.44	0.707
15	454.69	512.98	543.66	641.27	58.29	0.128	0.597	3.93	0.45	0.709
20	458.96	520.3	550.41	642.63	61.34	0.134	0.665	4.02	0.50	0.714
25	462.56	526.95	565.76	646.77	64.39	0.139	0.795	5.40	0.54	0.715
30	465.04	535.38	572.41	652.42	70.34	0.151	0.879	5.60	0.60	0.713

The glass transition and crystallization molar fractions (α) in the glass transition and crystallization regions, respectively are shown in Fig. 3. As mentioned above, the glass transition molar fraction and the crystallization molar fraction confirm that the tested samples are thermally active.

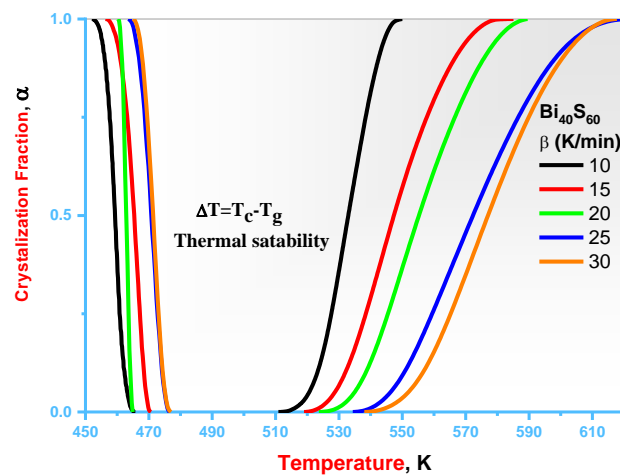


Fig. 3: The volume fraction α , for glass transition and crystallization phase as a function of temperature at different heating rates

4.2 Thermal stability studies

Various methods for studying the degree of glass stability based on characteristic temperatures obtained from DSC curves, such as T_g , T_p and melting temperature (T_m). Sakka and Mackenzie [xxii] have studied the glass thermal stability of various

compounds using the ratio (T_g/T_m). Moreover, the glass criterion [$\Delta T = (T_c - T_g)$] is an important parameter that gives information about the glass stability and glass forming ability [xxiii]. The greater value of ΔT implies more restricted crystallization process. Using the above characteristic temperatures, Hruby developed the H_r criterion, $H_r = \Delta T / (T_m - T_p)$. On the basis of the H_r criterion, Saad and Poulain [xxiv] obtained two other criteria, weighted thermal stability $H (= \Delta T / T_g)$ and S criterion [$= \Delta T (T_p - T_c) / T_g$]. The value of H_r reveals information about the probability of glass formation.

Dependence of the thermal stability parameters (ΔT , H_r , H and S), based on the characteristic temperatures (T_g , T_c , T_p and T_m), on the heating rate are shown in Fig. 4 (a&d). This figure shows that a linear relationship dependence of ΔT , H_r , H and S on heating rate β , which are the stability parameters, increases with increase in heating rate. These parameters allow predicting the glass forming ability such that materials with larger values of these parameters normally have greater glass thermal stability.

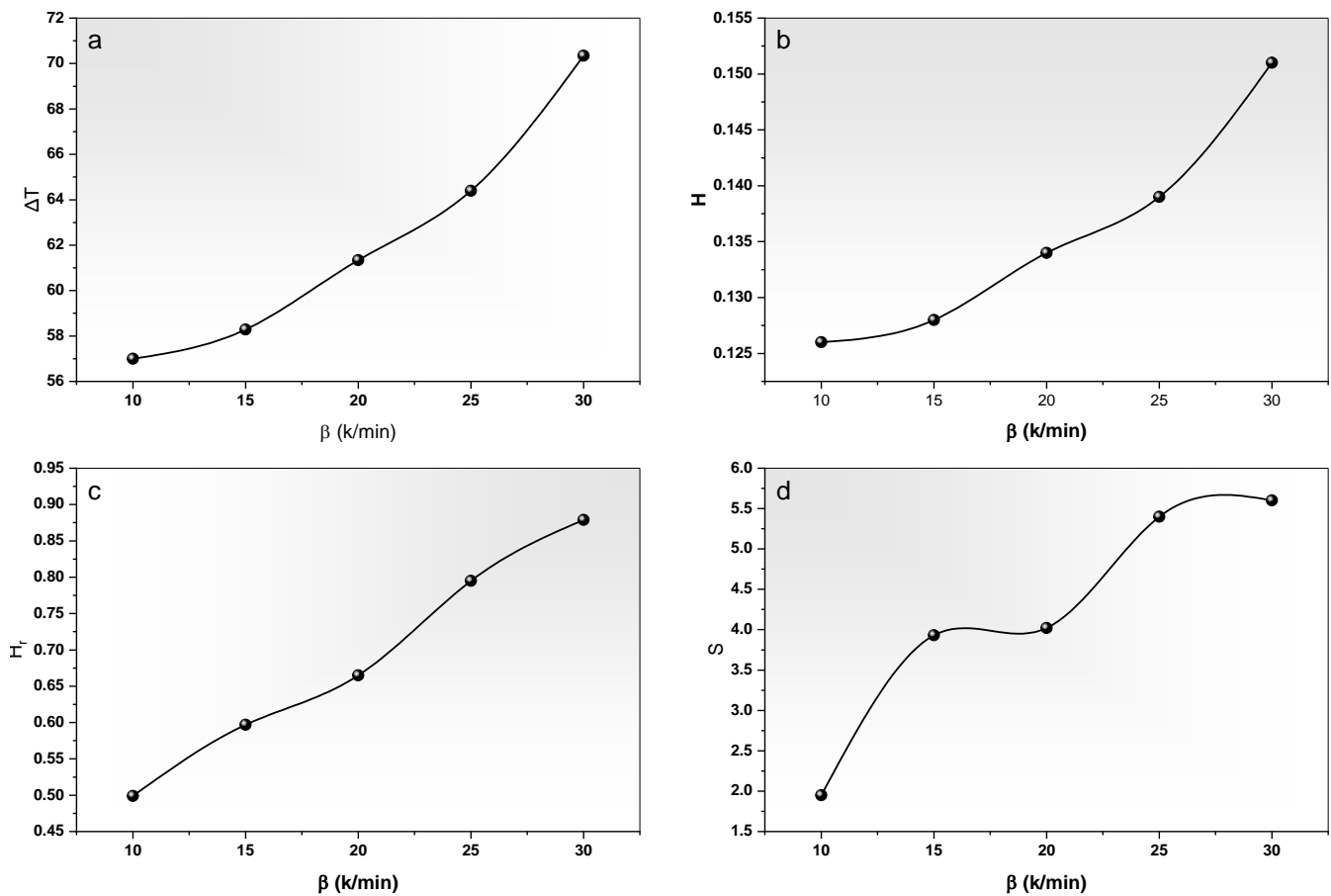


Fig. 4: Variation of the thermal stability parameters (ΔT , H_r , H and S), as a function of the heating rate (β) for Bi_2S_3 chalcogenide glass

4.3 Glass transition activation energy

A two-pronged approach could be used to examine the dependence between T_g and heating rate. Firstly, there is the empirical relationship proposed by Lasocka [xxv]

$$T_g = A_g + B_g \ln \beta \tag{14}$$

In this equation, A_g and B_g are constants that are dependent on the composition of the glass. B_g indicates the temporal response to configurational changes within the glass transition region, whereas A_g indicates the T_g at a heating rate of 1 K/min. The values of A_g and B_g can be estimated for the studied system by plotting of T_g versus $\ln \beta$, as shown in Fig. 5 (a). The obtained

values of A and B are 420.22 K and 13.06, respectively. Determining the glass transition activation energy E_t is the second method. The E_t of the studied glass alloys was calculated using the Kissinger method [16]:

$$\ln\left(\frac{\beta}{T_g^2}\right) = -\frac{E_t}{RT_g} + Const. \quad 15$$

The plots of $\ln(\beta/T_g^2)$ versus $1000/T_g$ for Bi_2S_3 chalcogenide glasses are shown in Fig. 5 (b). A value of 124.18 KJ/mol is estimated as the average activation energy for the glass transition.

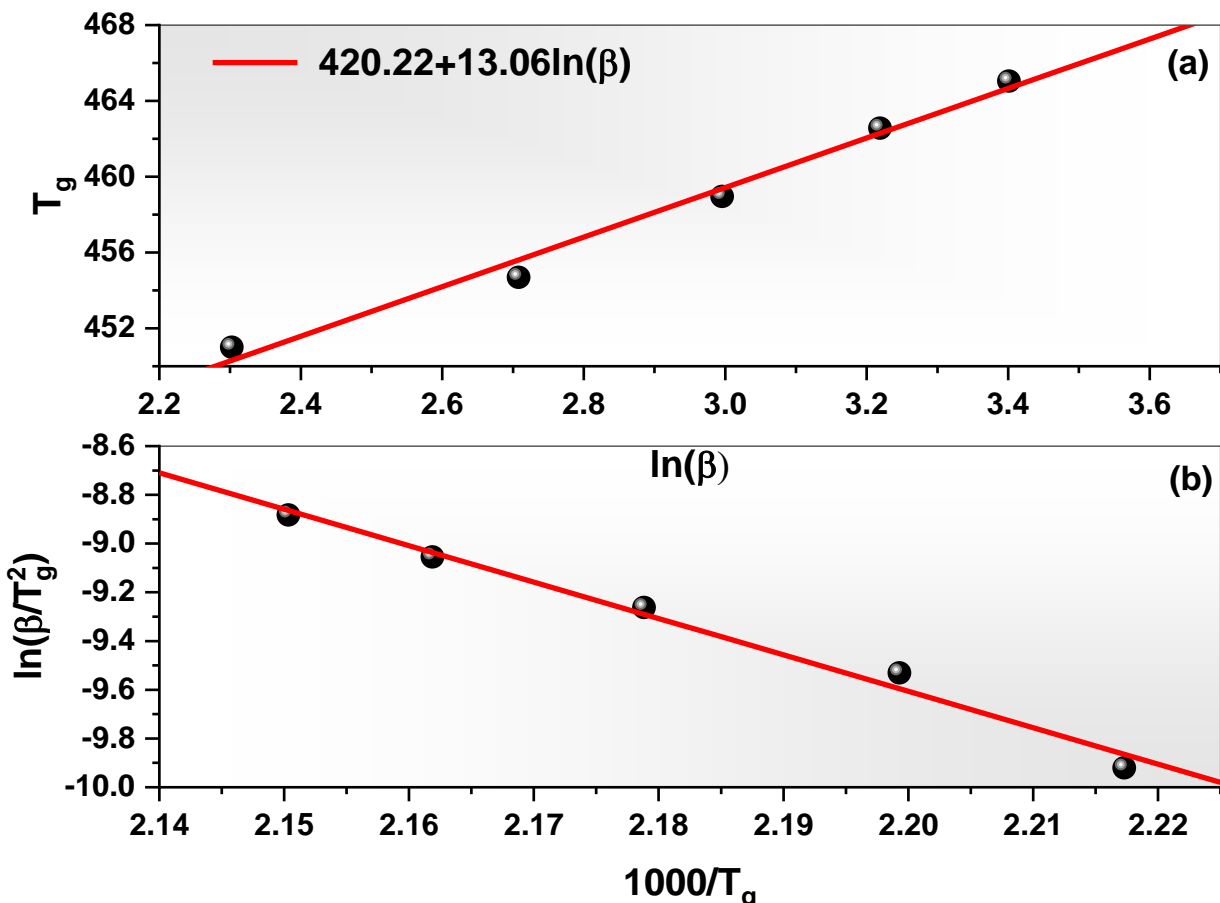


Fig. 5: (a) Glass transition temperature (T_g) versus $\ln(\beta)$ and (b) The plots of $\ln(\beta/T_g^2)$ versus $1000/T_g$ for Bi_2S_3 chalcogenide glasses

4.4 Estimation of Crystallization activation energy by isoconversional methods

Crystallization activation energy depends on the extent of conversion and the temperature. Using the experimental data provided in Fig. 3, we have applied different isoconversional methods, such as KAS, FWO, Tang, Starink, and Vyazovkin, to investigate the variation in activation energy. In these isoconversional methods, activation energies are evaluated for various values of α . The effective crystallization energy can be determined according to KAS, FWO, Tang, and Starink (linear method) (Figure 10) by plotting $\ln(\beta/T^2)$ versus $1000/T$, $\ln(\beta)$ versus $1000/T$, $\ln(\beta/T^{1.894661})$ versus $1000/T$ and $\ln(\beta/T^{1.92})$ versus $1000/T$, respectively (Figure 10). For all methods, straight lines were observed, which are in good agreement with Equations (8–11). Furthermore, the activation energy can be determined from the slope values. The activation energy required to crystallize the composition using different methods decreases with increasing crystallization fraction as can be seen in Fig. 6.

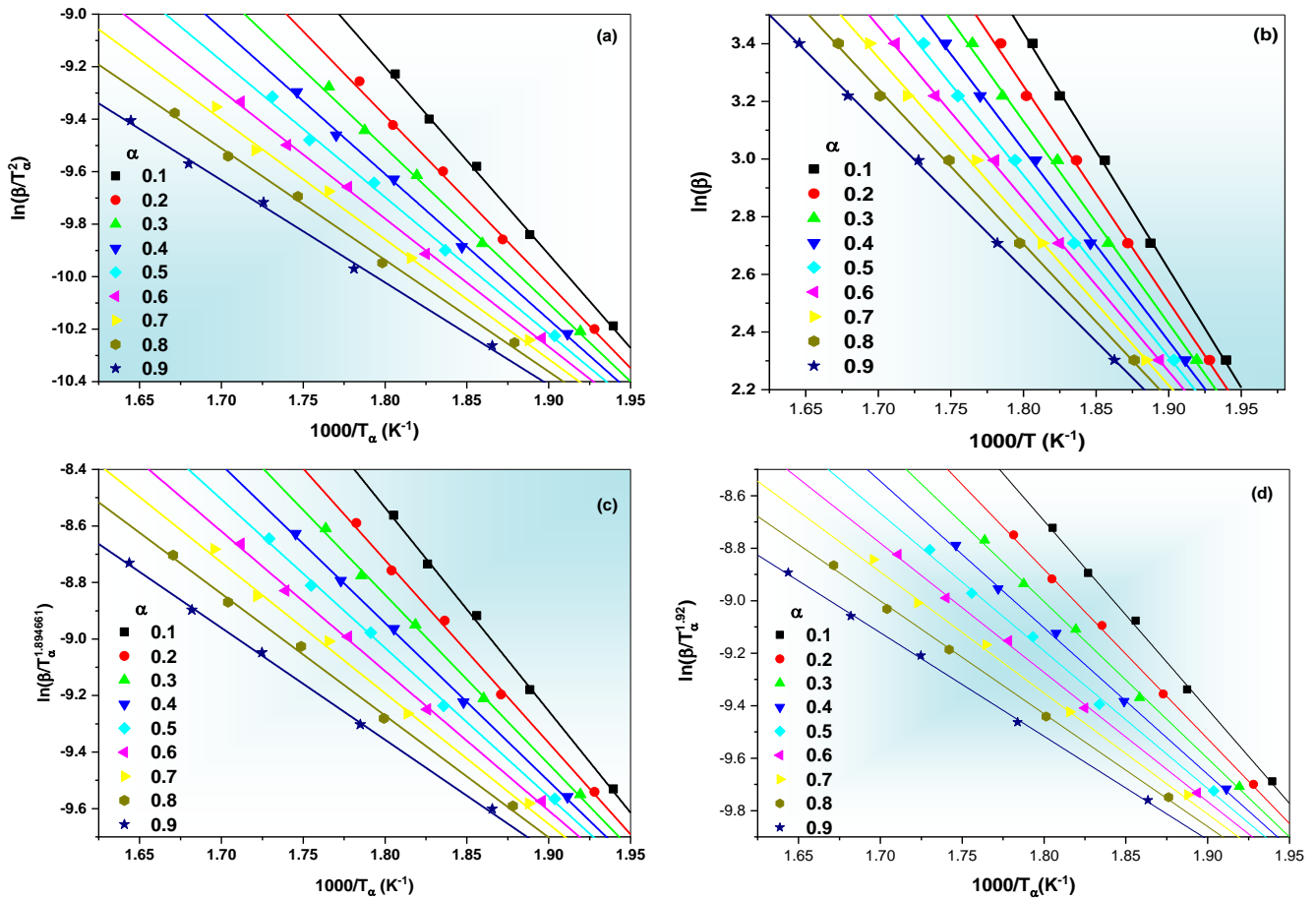


Fig. 6: Plots show (a) $\ln(\beta/T^2)$ versus $1000/T_p$, (b) $\ln(\beta)$ versus $1000/T$, (c) $\ln(\beta/T^{1.92})$ versus $1000/T$ and (d) $\ln(\beta/T^{1.894661})$ versus $1000/T$ (for $\alpha = 0.05, 0.25, 0.50, 0.75$ and 0.95) for the studied system. The straight lines are fit to (a) Kissinger-Akahira-Sunose equation, (b) Flynn-Wall-Ozawa equation, (c) Starink equation, and (d) Tang equation.

The Vyazovkin method, which is a nonlinear method, can also be used to calculate the effective activation energy of crystallization. In accordance with this approach, **Fig.7 (a)** depicts the parabolic curve between the minimization factor (Ω) and the effective activation energy of crystallization (E) for various crystallization fractions (0.05, 0.25, 0.5, 0.75, and 0.95). The value of effective activation energy corresponds to the inserted arrows in Figure 11 and to Equations (11 and 12), which were determined at a minimum value of Ω . For crystallization fractions of 0.05, 0.25, 0.5, 0.75, and 0.95, the activation energies at a minimum value of Ω are 150.54, 143.2, 138.52, 133.6, and 122.59 kJ/mol, respectively. The effective activation energy decreases with increasing A according to the five isoconversional transformation methods, as shown in **Fig. 7(b)**, while the KAS, Tang, Starink, and Vyazovkin methods produce identical results. The E_a found using the FWO approach is 3% higher than that found using the other methods. The effective activation energy only slightly changes when $0.3 \leq \alpha \leq 0.7$. **Fig. 7(b)** demonstrates that the transition from amorphous to crystalline materials cannot be explained by a single-step mechanism but by complicated multi-step reactions involving multiple growth processes with various activation energies and mechanisms.

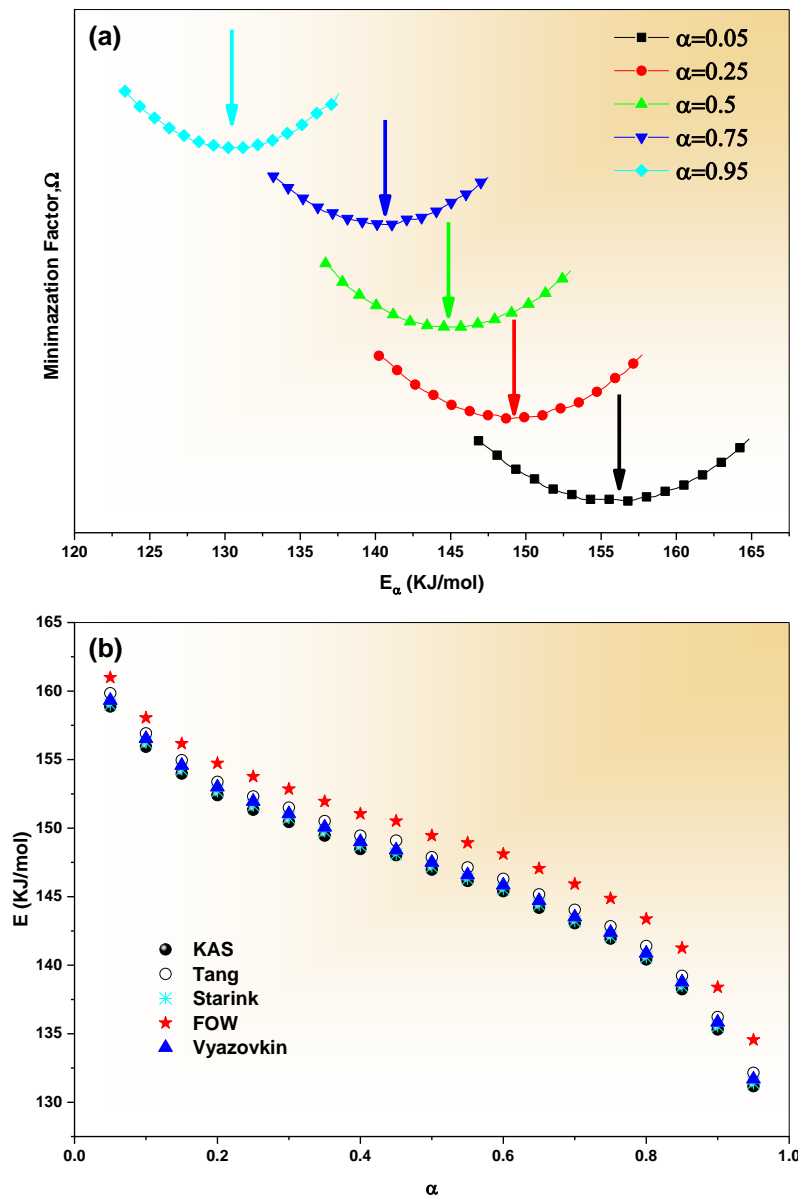


Fig. 7: (a) The minimization factor (Ω) against the activation energy for crystallization (E_{α}) at $\alpha = 0.05, 0.25, 0.50, 0.75$ and 0.95 (b) The effective activation energy (E) as a function the fractional conversion (α) as determined using different isoconversional methods for Bi_2S_3 composition

5. Conclusion

A kinetic study of Bi_2S_3 chalcogenide glass under nonisothermal conditions at different heating rates (10-30 K/min) was carried out. From DSC curves at various heating rates, characteristic temperatures such as glass transition temperature, crystallization peak start temperature, and thermal stability characteristics are determined. The activation energy required for the glass transition is calculated to be 124.18 kJ/mol. Furthermore, the crystallization activation energy is determined using several isoconversional techniques such as KAS, Tang, Starink, FWO and Vyazovkin. The results showed that the effective activation energy is not constant but varies with crystallization degree, and its value determined using the FWO method is 3% greater than that found using the other methods. The current study demonstrates that the transition of the Bi_2S_3 from the amorphous to the crystalline phase is a complicated process involving many mechanisms of nucleation and growth.

REFERENCES

- i) R. Sakthivel, S. Kubendhiran, S.-M. Chen., Ultrason. Sonochem. 54 (2019) 68.
- ii) X.-H. Liao, H. Wang, J.-J. Zhu, H.-Y. Chen., Mater. Res. Bull. 36 (2001) 2339.
- iii) C.D. Lokhande, Mater. Chem. Phys. 27 (1991) 1.
- iv) N. Parhi, B.B. Nayak, B.S. Acharya, Thin Solid Films 254 (1995) 47.
- v) Bhattacharya R. N. and Pramanik P., J. Electrochem. Soc. 129, (1982) 332.
- vi) Glatz A. C. and Meikleham V. F., J. Electrochem. Soc. 110, (1963)1231
- vii) Nair P. K. and Nair M. T. S., Semicond. Sci. Technol. 7, (1992) 239.
- viii) Vyazovkin S., New J Chem. 24(11)(2000) 913.
- ix) M. E. Rincon, Radl Suarez and P. K. Nair, J. Phys. Chem Solids 57:12 (1996) 1947.
- x) S. Vyazovkin, N. Sbirrazzuoli, Macromol. Rapid Commun. 23 (2002) 766.
- xi) S. Vyazovkin, N. Sbirrazzuoli, Macromol. Rapid Commun. 25 (2004) 733.
- xii) A. Khawam, D. R. Flanagan, Thermochim. Acta 436 (2005) 101.
- xiii) M.J. Starink, J. Mat. Sci. 42 (2007) 483.
- xiv) A. Khawam and D. R. Flanagan, *J. Phys. Chem. B* , 110:35 (2006) 17315.
- xv) M. J. Starink, Thermochim Acta. 2003;404(1-2):163-176.
- xvi) H.E. Kissinger, J. Res. Nat. Bureau Standards 57 (1956) 217.
- xvii) T. Akahira, T. Sunose, Res. Report Chiba Inst. Technol. 16 (1971) 22.
- xviii) J.H. Flynn, L.A. Wall, J. Res. Natl. Bur. Stand. Sect. A 70 (1966) 487.
- xix) T. Ozawa, Bull. Chem. Soc. Japan 38 (1965) 1881.
- xx) W. Tang, Y. Liu, H. Zhang, C. Wang, Thermochim. Acta 408 (2003) 39.
- xxi) S. Vyazovkin, N. Sbirrazzuoli, J Therm Anal Calorim., 2003;72(2):681-686.
- xxii) S. Sakka, J.D. Mackenzie, J. Non-Cryst. Solids 6 (1971) 145.
- xxiii) A. Dahshan, J. Non-Cryst. Solids 354 (2008) 3034.
- xxiv) M. Saad, M. Poulain, Mater. Sci. Forum 19 & 20 (1987) 11.
- xxv) M. Lasocka, Mater. Sci. Eng. 23 (1976) 173.

Citation of this Article:

Abdullah Omar Ali, Tawfik Mahmood Mohammed Ali, Mehdi Ahmed Dabban, "Determination of Activation Energy of Amorphous to Crystalline Transformation for Bi₂S₃ chalcogenide Glasses by Using Isoconversional Methods" Published in *International Current Journal of Engineering and Science - ICJES*, Volume 2, Issue 3, pp 10-20, July 2023.
